nature nanotechnology

LETTERS

PUBLISHED ONLINE: 28 FEBRUARY 2010 | DOI: 10.1038/NNANO.2010.17

Lipid multilayer gratings

Steven Lenhert[1,2,3]*, Falko Brinkmann[1,2], Thomas Laue[1], Stefan Walheim[1,4], Christoph Vannahme[5], Soenke Klinkhammer[6], Miao Xu[1], Sylwia Sekula[1], Timo Mappes[5], Thomas Schimmel[1,4] and Harald Fuchs[1,2,7]

The interaction of electromagnetic waves with matter can be controlled by structuring the matter on the scale of the wavelength of light, and various photonic components have been made by structuring materials using top-down or bottom-up approaches[1–5]. Dip-pen nanolithography is a scanning-probe-based fabrication technique that can be used to deposit materials on surfaces with high resolution and, when carried out in parallel, with high throughput[6–8]. Here, we show that lyotropic optical diffraction gratings—composed of biofunctional lipid multilayers with controllable heights between ∼5 and 100 nm—can be fabricated by lipid dip-pen nanolithography. Multiple materials can be simultaneously written into arbitrary patterns on pre-structured surfaces to generate complex structures and devices, allowing nanostructures to be interfaced by combinations of top-down and bottom-up fabrication methods. We also show that fluid and biocompatible lipid multilayer gratings allow label-free and specific detection of lipid–protein interactions in solution. This biosensing capability takes advantage of the adhesion properties of the phospholipid superstructures and the changes in the size and shape of the grating elements that take place in response to analyte binding.

Fundamental photonic components can be generated from a large variety of materials by top-down lithography or bottom-up self-assembly. Examples include simple Bragg gratings[1], stacks[2] and two- or three-dimensional photonic materials[3–5]. A major challenge lies in the integration of multiple chemical functionalities for the generation of more complex devices, including the readout system, in a simple and efficient way. Top-down microfabrication strives to fabricate smaller structures from a single material, whereas the bottom-up approach seeks to assemble and integrate small components into larger and more complex devices. Dip-pen nanolithography (DPN) is a unique method of micro- and nanofabrication, as it is a direct-write method that allows the bottom-up integration of a variety of materials (especially organic and biological molecules) with both high resolution and high throughput[7,8].

Phospholipids are fundamental structural and functional components of biological membranes that are both fluid and responsive to external stimuli[9]. In the presence of water, phospholipids spontaneously self-organize to form liposomes (or vesicles), which are widely used for a variety of biological and nanotechnological applications. For example, the physical chemistry of liposome adhesion on surfaces is well studied as a model system for cell-surface interactions and surface biofunctionalization in general[10]. Furthermore, liposomes have been used as nanoscale containers with attolitre to zeptolitre volumes and networks for nanoscale transport of materials between vessels[11,12]. The loading of vesicles (for example, by surface binding, encapsulation or intercalation) with a variety of biofunctional materials such as drugs, nucleic acids and proteins is developed for applications in delivery to biological cells[13,14]. The structuring of adherent phospholipid multilayers into arbitrary photonic structures described here therefore provides a new approach for the fabrication and observation of biomimetic nanosystems.

Fluid phospholipids such as 1,2-dioleoyl-*sn*-glycero-3-phosphocholine (DOPC) are particularly well suited as biocompatible inks for DPN because their viscosity, and corresponding properties of ink transport between the DPN tip and substrate, can be readily tuned by the relative humidity[15]. They can therefore be used to write on a variety of solid substrates (possibly pre-patterned) without a specific chemical driving force or covalent binding to the surface. Because they are biological molecules, a variety of functional membrane lipids (both natural and synthetic) are readily available and can be directly dispersed in the ink for the fabrication of biofunctional structures. These different biofunctions can then be simultaneously written onto the same substrate using different tips in a parallel array, for example, by microfluidic inkwells or inkjet printing, a method referred to as multiplexed DPN[16,17]. Importantly, the self-organization properties of phospholipids enable them to stack controllably into multilayer structures that are used for optical diffraction, as shown schematically in Fig. 1. The ability of lipid DPN to control the lipid multilayer height constructively[15] is crucial to this development. With the exception of capillary assembly[18], the majority of lipid patterning methods are limited to single monolayers or surface-supported lipid bilayers[19].

The quality of the structure can be rapidly characterized by illumination of the patterns in a way that allows observation of the diffraction from gratings over large areas (Fig. 2), which can also be carried out *in situ* during DPN fabrication, allowing rapid prototyping of photonic structures. For example, in Fig. 2a, the period of the gratings was varied between 500 and 700 nm, and the diffracted light of different colours was detected by a simple charge-coupled device (CCD) camera (optical spectra of the diffracted light are shown in Supplementary Fig. S1). The different colours observed as a function of grating pitch are described by the grating equation $d(\sin\theta_m + \sin\theta_i) = m\lambda$, where d is the period of the grating, θ_m and θ_i are the angles of diffraction maxima and incidence, respectively, m is the diffraction order, and λ is the wavelength of light. In our set-up, we use white incident light and observe the intensity of light at $\theta_m \approx 0^\circ$ normal to the grating plane. The colour observed depends only on the grating period and θ_i, which are adjusted to give optimal contrast with a period of 600 nm illuminated at $\theta_i \approx 70^\circ$.

[1]Institute of Nanotechnology, Karlsruhe Institute of Technology, 76021 Karlsruhe, Germany, [2]Physikalisches Institut, Westfälische Wilhelms-Universität, and Center for Nanotechnology (CeNTech), 48149 Münster, Germany, [3]Department of Biological Science and Integrative NanoScience Institute, Florida State University, Tallahassee, Florida 32306-4370, USA, [4]Institute of Applied Physics, Center for Functional Nanostructures (CFN), Karlsruhe Institute of Technology, 76128 Karlsruhe, Germany, [5]Institut für Mikrostrukturtechnik, Karlsruhe Institute of Technology, 76128 Karlsruhe, Germany, [6]Light Technology Institute, and Center for Functional Nanostructures (CFN), Karlsruhe Institute of Technology, 76128 Karlsruhe, Germany, [7]Department of Nanobio Materials and Electronics, Gwangju Institute of Science and Technology, Gwangju, Korea. *e-mail: lenhert@bio.fsu.edu

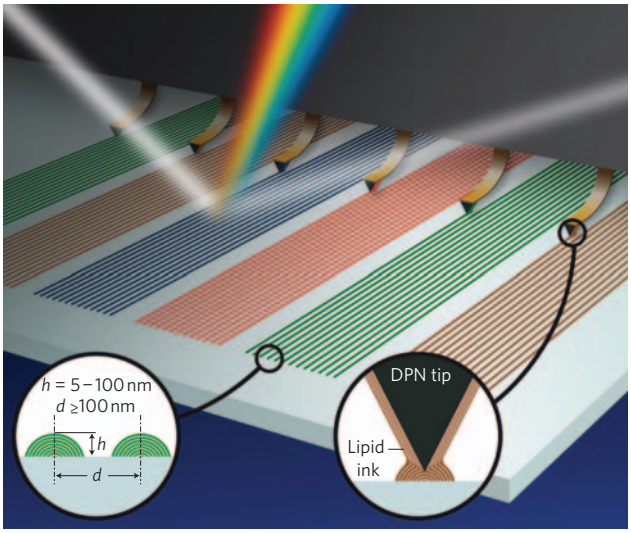

Figure 1 | Schematic of the technique used to fabricate lipid multilayer gratings. Parallel DPN tip arrays are used to deposit multiple lipids simultaneously with controllable multilayer heights, laterally structured to form arbitrary patterns (for example, diffraction gratings) with feature sizes on the same scale as UV, visible or infrared light. *In situ* observation of the light diffracted from the patterns can be carried out during DPN and used for high-throughput optical quality control without the need for fluorescence labels.

Correlating the grating topographies measured by atomic force microscopy (AFM) with the intensity of light diffracted from the gratings into the camera permits calibration of the observed diffraction intensities (Fig. 2b,c). Figure 2c shows that, for gratings with a period of 600 nm and ink composed of the pure DOPC, the intensity of diffracted light increases linearly with grating height up to 40–60 nm and then discontinuously drops off for thicker gratings (because, beyond that height, the grating lines fuse together to form a continuous film; Supplementary Fig. S2). The variation in height along a single line is ~10% of the grating height (Supplementary Fig. S3).

The constructive and parallel nature of DPN makes it uniquely capable, at present, of integrating multiple materials on surfaces that have been pre-structured by top-down lithographic methods for complex device fabrication. As an example, we fabricated functional waveguide grating couplers[20] by direct DPN patterning of DOPC multilayer gratings onto waveguides as shown in Fig. 3. The waveguides were formed on poly(methyl methacrylate) (PMMA) surfaces by exposure to deep ultraviolet light through a chromium mask[21]. A lipid grating with a period of 700 nm was defined on top of the UV-induced PMMA waveguide with the lines perpendicular to the waveguide. Light from a supercontinuum laser source (Koheras SuperK Versa) with a spectral emission range of $\lambda = 500–800$ nm was coupled into the waveguide through an optical fibre. Supercontinuum laser light of different wavelengths was decoupled under different angles by the grating coupler, as shown in Fig. 3b,c and Supplementary Video S1.

Advanced photonics applications demand the integration of multiple functional materials on micro- and nanoscopic scales and in arbitrary geometries[22,23]. To demonstrate the qualitatively unique ability of DPN to address this challenge, we used multiplexed DPN[17] to write two different fluorescently labelled lipids simultaneously on pre-structured waveguides. Figure 3d shows two different gratings simultaneously fabricated from two different tips in a parallel array dipped in inks doped with 1 mol% of

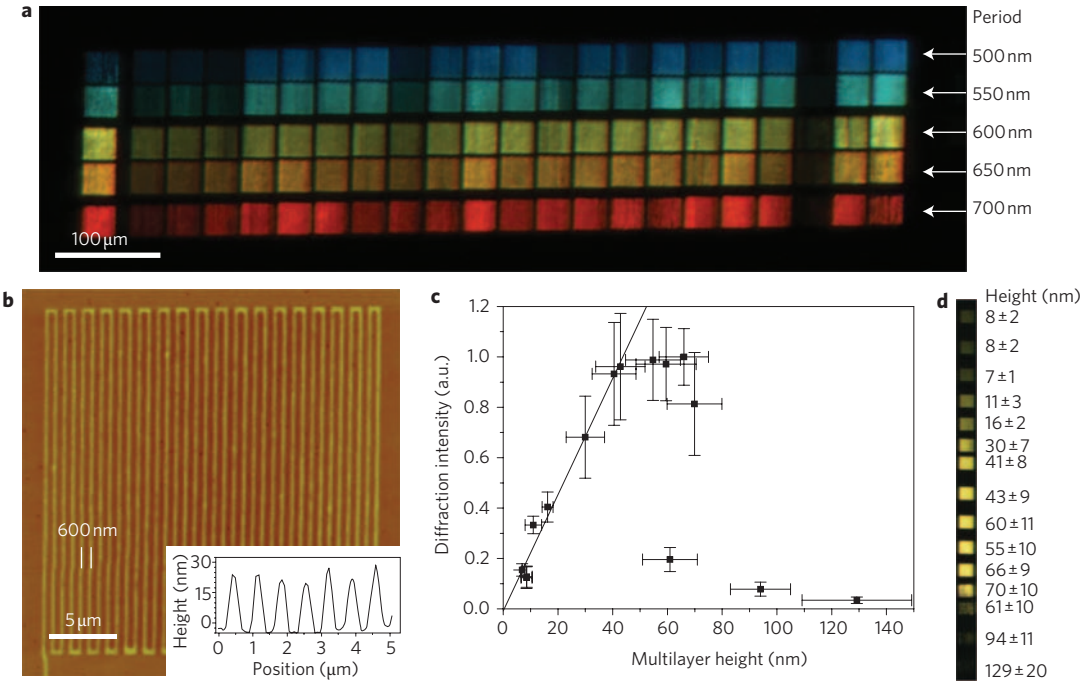

Figure 2 | Optical and topographical characterization of the gratings. a, Optical micrograph of light diffracted from gratings of different period that were fabricated in parallel with a one-dimensional tip array[35] on a poly(methyl methacrylate) surface. Each tip wrote five gratings with periods ranging from 500 to 700 nm in steps of 50 nm (top to bottom). **b**, AFM topographical image of a grating with a period of 600 nm and height of (29±3) nm. **c**, Correlation between the grating heights (measured by AFM) and the measured intensity of light diffracted from gratings with a period of 600 nm. The grating efficiency steadily increases linearly to heights of (50±10) nm, after which the multilayer patterns fuse to form a continuous film that no longer diffracts light. A line is fit to the linear region of the data and can be used for optical calibration of the heights. Error bars for the height measurement represent the standard deviation in heights between different grating lines. **d**, Optical micrograph of the diffraction from the gratings in **c** and their measured AFM heights.

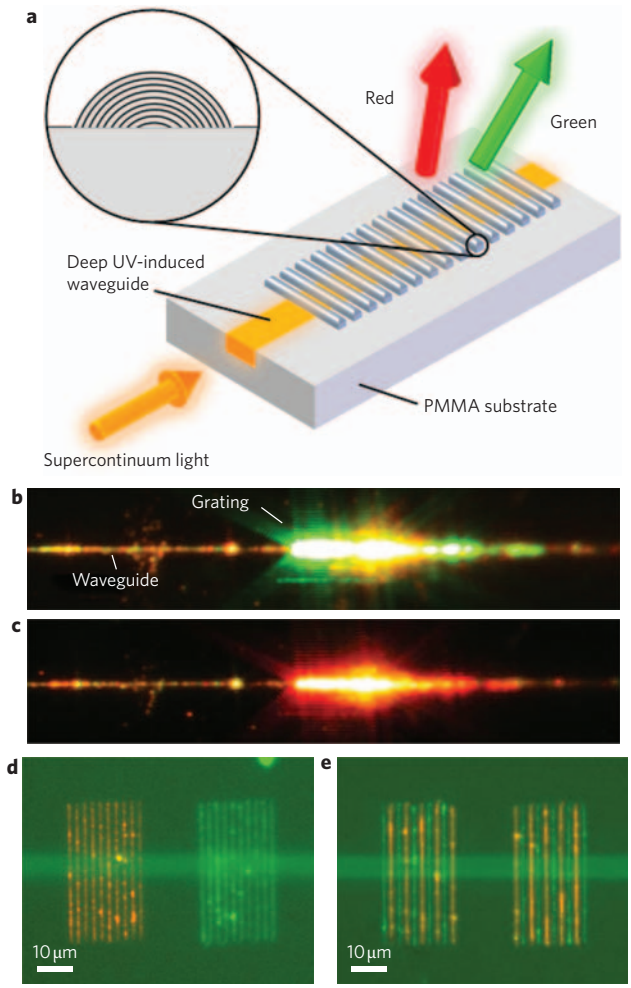

Figure 3 | Bottom-up and top-down integration of multimaterial waveguide grating couplers. a, Schematic of the waveguide grating couplers. Light of a supercontinuum laser source is coupled into a single-mode strip waveguide and decoupled by the grating coupler. **b**,**c**, Photographs of the coupler at 30° and 45° from the surface normal, where the red and green portions of the guided supercontinuum light are coupled to radiation modes, respectively. **d**,**e**, Fluorescence overlay of red and green fluorescence from two different fluorescently labelled lipids (red and green vertical lines) integrated with a pitch of 2 μm by DPN patterning on a waveguide (horizontal green line visible because of autofluorescence).

fluorescently labelled lipids—rhodamine (red) and fluorescein (green). Figure 3e shows two more gratings made with the same tip array and inks, where the individual elements within a single grating are composed of alternating materials. This capability of DPN to control the placement of different materials selectively within a structure opens new possibilities for the rapid prototyping and fabrication of multicomponent photonic structures.

Finally, the structuring of lipids into photonic structures provides a label-free method of observing dynamic structural changes in the lipid multilayer morphologies. These changes can be understood in terms of liquid adhesion to a solid surface where the lipid multilayers are essentially structured micro- and nanoscopic oil droplets adherent on a surface[24]. Three examples of shape changes that we have observed are spreading, dewetting and intercalation of materials into the multilayer structure, as schematically illustrated in Fig. 4a. The drawings in Fig. 4a have been sketched to reflect the well-documented tendency for hydrated phospholipid multilayers to stack on surfaces into ordered multilamellar bilayer stacks[25] and for hydrophilic materials to intercalate themselves between the hydrophobic multilayer sheets[14].

When patterned on surfaces, lipid multilayers are known to spread spontaneously in aqueous solution to form lipid bilayer or monolayer precursor films on certain substrates[15,26–28]. In air, the phospholipid DOPC undergoes a hydration-induced gel-fluid phase transition at a relative humidity of 40%, as observed by humidity-controlled calorimetry and DPN[15,29]. The multilayer gratings therefore remain stable for long-term storage at low humidity, but upon exposure to humidity higher than 40% in air, the multilayers become hydrated and fluid and therefore slowly spread on the surface. This spreading can be observed both by fluorescence microscopy in Fig. 4a and as a decrease in the diffraction intensity (Supplementary Fig. S4b), irreversibly indicating the presence of water vapour above 40% humidity.

Surprisingly, lipid multilayer gratings can remain stable in aqueous solution for at least several days when immersed under the appropriate conditions (Supplementary Fig. S5), permitting study of the structural changes upon binding of biological molecules such as proteins, which we have seen to result in the dewetting and intercalation effects observed by fluorescence microscopy and shown in Fig. 4c,d. For this purpose, we doped the DOPC ink with 5 mol% of a biotinylated lipid. The chemical structures of these lipids are shown Fig. 4e. Fluorescently labelled lipids reveal the multilayer grating lines to break into droplets upon exposure to 50 nM of the tetravalent biotin-binding protein streptavidin (Supplementary Video S2 and Fig. S6). Such dewetting or formation of droplets from a continuous line drawn on a surface by a pen is a common practical method of characterizing surface energies by means of dyne pens[30], and here we extend this method to the nanoscale. A semi-empirical model of the dewetting based on a change in droplet height as a result of increased surface tension of the oil–water interface (for example, upon protein binding) is presented in Supplementary Fig. S7.

Using both fluorescently labelled proteins and lipids, we were able to observe intercalation of the proteins into lipid multilayers. For example, in the experiment in Fig. 4d, lines of different multilayer heights were drawn with DOPC containing both a fluorescein-labelled lipid and a biotinylated lipid, as indicated by the different intensities of the fluorescence from the different lines in the green, 'before' image of Fig. 4d. Upon binding of Cy3-labelled protein (red and green overlay image in Fig. 4d), the higher lines can be seen to be significantly brighter than the lower lines, suggesting intercalation into the multilayers after incubation for 1 h. Further experiments using fused biotinylated squares of different heights to bind streptavidin (Supplementary Fig. S8), as well as the use of his-tagged green fluorescent protein (GFP) to bind to gratings doped with his-tag binding lipids, confirm the ability of proteins to intercalate themselves within the multilayers (Supplementary Fig. S9).

The tendency for the lipid grating elements to change size and shape upon protein binding, in combination with their optical properties and innate biofunctions, opens the possibility of a new, biologically inspired mechanism for label-free protein detection. Grating-based biosensors are well established and typically function by detecting a spectral change upon analyte binding to the surface of a biofunctionalized solid grating[31–33]. Although the vast majority of such sensors are made of solid materials, liquid diffraction gratings formed from the directed condensation of water droplets onto chemically patterned surfaces have been proposed as humidity sensors as well as for fundamental studies in adhesion science[34]. The lipid gratings described here differ from the existing grating-based sensors described above in two aspects. First, the biofunctions can be incorporated directly into the phospholipid ink, eliminating the need for further biofunctionalization steps of the transducer as in the case of existing solid gratings. Second, in contrast to the

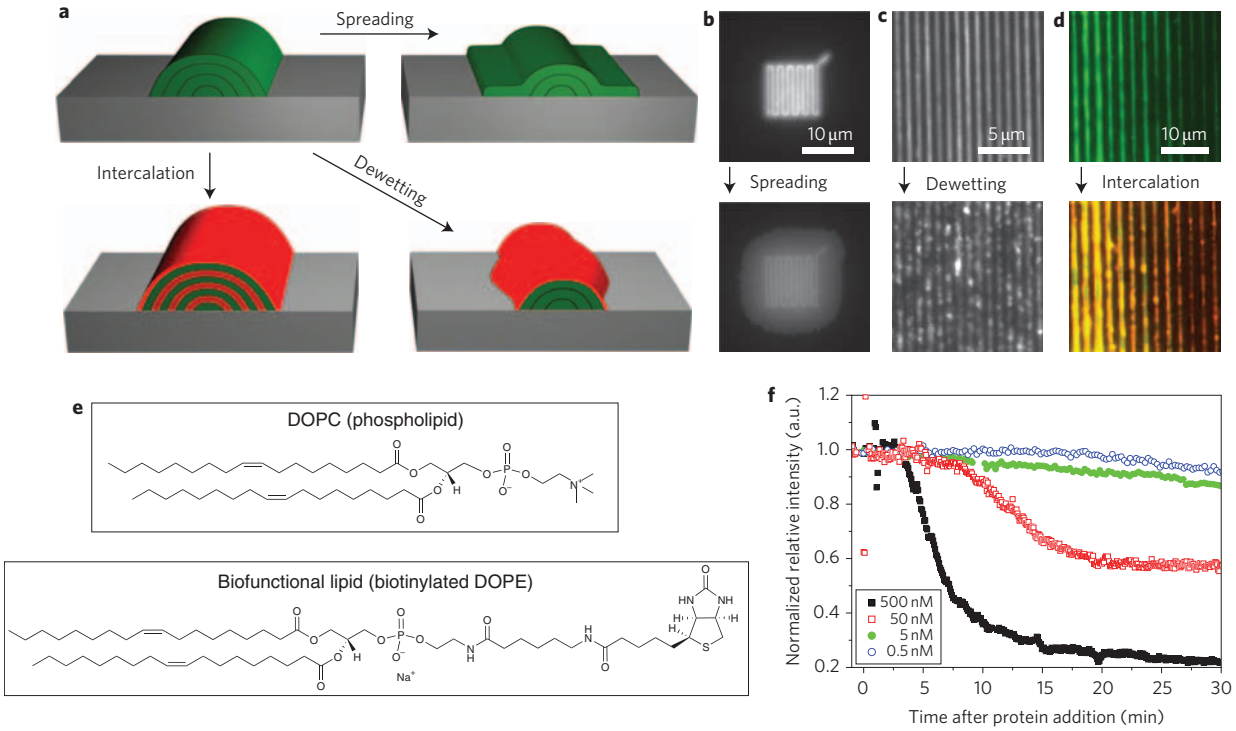

Figure 4 | Lipid nanodynamics and protein detection. a, Schematics of the three effects observed here as a result of lipid adhesion with the substrate and interaction with protein from solution. Green represents the lipid multilayers and red the protein. **b–d**, Fluorescence micrographs made with fluorescently labelled materials for observation of the dynamic processes: lipid spreading in air after 5 min of exposure to humidity above 40% (**b**); dewetting of smooth lines of biotin-containing gratings under solution to form droplets after 1 min of exposure to the protein streptavidin (**c**); intercalation of protein into lipid multilayer grating lines of different heights after 1 h (**d**). The top image is a fluorescence micrograph of fluorescein- (green) labelled lipid grating lines before exposure to protein, and the bottom image shows an image of both red and green fluorescence channels overlaid after binding of a Cy3- (red) labelled protein bound to the layers. Intercalation is indicated because the intensity of fluorescence from bound protein is proportional to the height of the lipid multilayer. **e**, Chemical structures of phospholipids (1,2-dioleoyl-*sn*-glycero-3-phosphocholine (DOPC) and the biotinylated lipid 1,2-dioleoyl-*sn*-glycero-3-phosphoethanolamine-*N*-(cap biotinyl)) used as the DPN inks for fabricating biotinylated gratings for detection of the biotin-binding protein streptavidin, in parallel with control gratings composed of pure DOPC. **f**, Label-free detection of protein binding by monitoring of the diffraction from gratings upon exposure to protein at different concentrations. The decrease in diffraction intensity under these conditions is due to the dewetting mechanism.

condensation-based liquid gratings, the immiscibility of the adherent liquid phospholipid droplets with water permits studies in biologically relevant aqueous solutions[35].

Monitoring the intensity of light diffracted from lipid multilayer gratings on exposure to analytes permits optical detection of protein binding without any fluorescent labels. For example, Fig. 4f shows the optical response of biotinylated gratings upon exposure to streptavidin protein at different concentrations. The decrease in intensity is due to the dewetting mechanism, which results in a lower diffraction efficiency. Our limit of detection of 5 nM after 15 min is comparable to that of solid grating-based sensors, which are typically diffusion limited at concentrations on the order of ~5 nM (refs 31,32), but after incubation for 90 min, we are able to observe significant dewetting of biotinylated gratings, as compared to the pure DOPC control gratings, at a protein concentration of 500 pM (Supplementary Fig. S10). As the dewetting detection mechanism depends on a change in surface energy, the sensitivity for a particular analyte could be optimized by adjustment of the sensitivity of the membrane tension to ligand binding, as is the case in many cell-signalling processes and model membrane systems[11]. Furthermore, phospholipid bilayers are highly resistant to non-specific protein binding, and we were therefore able to carry out the same detection of protein added to fetal calf serum (Supplementary Fig. S11 and Video S3). The response of the grating to protein binding depends on the grating height; higher gratings give the best response for protein detection at low concentration (Supplementary Fig. S12). Therefore, observing a quantitative concentration-dependent response requires use gratings of equivalent height (35 ± 5 nm as determined by diffraction intensity calibration) for the experiment series shown in Fig. 4f.

Intercalation effects can also be observed by monitoring of diffraction and correspond to increases in the grating volume and therefore height (Supplementary Figs S9,S12). For example, in the case of streptavidin binding, dewetting and intercalation are observed simultaneously for higher gratings at higher concentrations (for example, 500 nM and above), whereas only intercalation is observed for the lower gratings (for example, Fig. 4d; see also Supplementary Fig. S12). At lower streptavidin concentrations, however, no response is observed for lower gratings, and only dewetting is observed for the higher gratings. Another demonstration of intercalation can be observed by diffraction on binding of a his-tagged GFP protein to nickel-chelating lipid gratings, where the diffraction intensity doubled (Supplementary Fig. S9). Upon addition of imidazole, which releases the his-tag-bound protein, the diffraction intensity could be seen to decrease, and the effect was reversible. Although intercalation and reversibility of the fluid grating response to analytes has so far only been observed for higher, millimolar concentrations, where new sensor constructs are hardly needed, the intercalation mechanism demonstrates the possibility of expanding the dynamic range of disposable sensors. Furthermore, the ability to observe analyte intercalation and desorption from lipid multilayers provides a new, label-free method

of characterizing loading and release conditions of liposomes for delivery and nanoscale chemistry applications.

In conclusion, we have developed a process for the fabrication of photonic structures composed of phospholipid multilayers. It allows direct writing of arbitrary patterns, composed of multiple biocompatible membrane-based materials, on a variety of surfaces, including pre-patterned substrates. The technique is useful for high-throughput biophysical analysis with lipid-based photonic structures and novel photonic sensing elements capable of label-free biosensing by means of a dynamic shape change upon analyte binding. Higher gratings that respond to analyte binding by a surface-tension change are found to be suitable for detection of analytes at low concentrations, whereas mechanisms based on intercalation of materials into the fluid gratings can expand the dynamic range of sensing as well as provide a new way to probe dynamic biomembrane function. The bottom-up fabrication method and unique biophysical properties of nanostructured lipid multilayers permits the integration of complex and dynamic biophotonic circuits.

Received 19 August 2009; accepted 22 January 2010; published online 28 February 2010

References

1. Rittenhouse, D. Explanation of an optical deception. *Trans. Am. Phil. Soc.* **2,** 37–42 (1786).
2. Choi, S. Y., Mamak, M., von Freymann, G., Chopra, N. & Ozin, G. A. Mesoporous Bragg stack color tunable sensors. *Nano Lett.* **6,** 2456–2461 (2006).
3. Joannopoulos, J. D., Villeneuve, P. R. & Fan, S. H. Photonic crystals: putting a new twist on light. *Nature* **386,** 143–149 (1997).
4. Ebbesen, T. W., Lezec, H. J., Ghaemi, H. F., Thio, T. & Wolff, P. A. Extraordinary optical transmission through sub-wavelength hole arrays. *Nature* **391,** 667–669 (1998).
5. Pendry, J. B., Schurig, D. & Smith, D. R. Controlling electromagnetic fields. *Science* **312,** 1780–1782 (2006).
6. Piner, R. D., Zhu, J., Xu, F., Hong, S. H. & Mirkin, C. A. 'Dip-pen' nanolithography. *Science* **283,** 661–663 (1999).
7. Ginger, D. S., Zhang, H. & Mirkin, C. A. The evolution of dip-pen nanolithography. *Angew. Chem. Int. Ed.* **43,** 30–45 (2004).
8. Salaita, K., Wang, Y. H. & Mirkin, C. A. Applications of dip-pen nanolithography. *Nature Nanotech.* **2,** 145–155 (2007).
9. Phillips, R., Ursell, T., Wiggins, P. & Sens, P. Emerging roles for lipids in shaping membrane-protein function. *Nature* **459,** 379–385 (2009).
10. Sackmann, E. Supported membranes: scientific and practical applications. *Science* **271,** 43–48 (1996).
11. Chiu, D. T. *et al.* Chemical transformations in individual ultrasmall biomimetic containers. *Science* **283,** 1892–1895 (1999).
12. Karlsson, A. *et al.* Molecular engineering—networks of nanotubes and containers. *Nature* **409,** 150–152 (2001).
13. Storm, G. & Crommelin, D. J. A. Liposomes: quo vadis? *Pharm. Sci. Technol. Today* **1,** 19–31 (1998).
14. Radler, J. O., Koltover, I., Salditt, T. & Safinya, C. R. Structure of DNA–cationic liposome complexes: DNA intercalation in multilamellar membranes in distinct interhelical packing regimes. *Science* **275,** 810–814 (1997).
15. Lenhert, S., Sun, P., Wang, Y. H., Fuchs, H. & Mirkin, C. A. Massively parallel dip-pen nanolithography of heterogeneous supported phospholipid multilayer patterns. *Small* **3,** 71–75 (2007).
16. Wang, Y. H. *et al.* A self-correcting inking strategy for cantilever arrays addressed by an inkjet printer and used for dip-pen nanolithography. *Small* **4,** 1666–1670 (2008).
17. Sekula, S. *et al.* Multiplexed lipid dip-pen nanolithography on subcellular scales for the templating of functional proteins and cell culture. *Small* **4,** 1785–1793 (2008).
18. Diguet, A., Le Berre, M., Chen, Y. & Baigl, D. Preparation of phospholipid multilayer patterns of controlled size and thickness by capillary assembly on a microstructured substrate. *Small* **5,** 1661–1666 (2009).
19. Sanii, B. & Parikh, A. N. Patterning fluid and elastomeric surfaces using short-wavelength UV radiation and photogenerated reactive oxygen species. *Annu. Rev. Phys. Chem.* **59,** 411–432 (2008).
20. Tamir, T. & Peng, S. T. Analysis and design of grating couplers. *Appl. Phys.* **14,** 235–254 (1977).
21. Henzi, P., Rabus, D. G., Bade, K., Wallrabe, U. & Mohr, J. Low cost single mode waveguide fabrication allowing passive fiber coupling using LIGA and UV flood exposure. *Proc. SPIE* **5454,** 64–74 (2004).
22. Abouraddy, A. F. *et al.* Towards multimaterial multifunctional fibres that see, hear, sense and communicate. *Nature Mater.* **6,** 336–347 (2007).
23. Bonifacio, L. D., Lotsch, B. V., Puzzo, D. P., Scotognella, F. & Ozin, G. A. Stacking the nanochemistry deck: structural and compositional diversity in one-dimensional photonic crystals. *Adv. Mater.* **21,** 1641–1646 (2009).
24. Mendez-Vilas, A., Jodar-Reyes, A. B. & Gonzalez-Martin, M. L. Ultrasmall liquid droplets on solid surfaces: production, imaging and relevance for current wetting research. *Small* **5,** 1366–1390 (2009).
25. Nagle, J. F. & Tristram-Nagle, S. Structure of lipid bilayers. *BBA Rev. Biomembranes* **1469,** 159–195 (2000).
26. Sanii, B. & Parikh, A. N. Surface-energy dependent spreading of lipid monolayers and bilayers. *Soft Matter* **3,** 974–977 (2007).
27. Nissen, J., Gritsch, S., Wiegand, G. & Radler, J. O. Wetting of phospholipid membranes on hydrophilic surfaces—concepts towards self-healing membranes. *Eur. Phys. J. B* **10,** 335–344 (1999).
28. Radler, J., Strey, H. & Sackmann, E. Phenomenology and kinetics of lipid bilayer spreading on hydrophilic surfaces. *Langmuir* **11,** 4539–4548 (1995).
29. Ulrich, A. S., Sami, M. & Watts, A. Hydration of DOPC bilayers by differential scanning calorimetry. *BBA Biomembranes* **1191,** 225–230 (1994).
30. Rentzhog, M. & Fogden, A. Print quality and resistance for water-based flexography on polymer-coated boards: dependence on ink formulation and substrate pretreatment. *Prog. Org. Coat.* **57,** 183–194 (2006).
31. Lai, Z. A., Wang, Y. L., Allbritton, N., Li, G. P. & Bachman, M. Label-free biosensor by protein grating coupler on planar optical waveguides. *Opt. Lett.* **33,** 1735–1737 (2008).
32. Fan, X. D. *et al.* Sensitive optical biosensors for unlabeled targets: a review. *Anal. Chim. Acta* **620,** 8–26 (2008).
33. Morhard, F., Pipper, J., Dahint, R. & Grunze, M. Immobilization of antibodies in micropatterns for cell detection by optical diffraction. *Sens. Actuat. B* **70,** 232–242 (2000).
34. Kumar, A. & Whitesides, G. M. Patterned condensation figures as optical diffraction gratings. *Science* **263,** 60–62 (1994).
35. Zhang, M. *et al.* A MEMS nanoplotter with high-density parallel dip-pen manolithography probe arrays. *Nanotechnology* **13,** 212–217 (2002).

Acknowledgements

The authors thank W. Schroeder for drawing Fig. 1, T. Heiler for Fig. 3a, and A.B. Thistle for editorial review. S.L. thanks S. Gaertner, M. Ruben and L.F. Chi for discussion. S.L. and H.F. thank the Deutsche Forschungsgemeinschaft (DFG, German Research Foundation, project FU 299/14-1) for financial support. S.S. and S.L. acknowledge funding from the DFG Center for Functional Nanomaterials (CFN E3.2). T.M.'s Young Investigator Group YIG 08 received financial support from the 'Concept for the Future' of Karlsruhe Institute of Technology within the framework of the German Excellence Initiative. C.V. and S.K. acknowledge financial support from the Karlsruhe School of Optics and Photonics.

Author contributions

S.L. conceived the study, coordinated experiments and wrote the paper. F.B. carried out the initial DPN and characterization, and T.L. advanced the sensing experiments with contributions from S.L., S.W., M.X. and S.S. The grating coupler was developed by C.V., S.K. and T. M. T.S. and H.F. contributed significantly to the scientific discussion of the project.

Additional information

The authors declare no competing financial interests. Supplementary information accompanies this paper at www.nature.com/naturenanotechnology. Reprints and permission information is available online at http://npg.nature.com/reprintsandpermissions/. Correspondence and requests for materials should be addressed to S.L.